NASA TECHNICAL MEMORANDUM

NASA TM X-71976

COPY NO.

NASA TM X-71976

THE EFFECT OF ABLATION INJECTION ON RADIATIVE AND CONVECTIVE HEATING

By James N. Moss

Langley Research Center
Hampton, Virginia

Presented at the 10th Anniversary Meeting of the Society of Engineering Science, 1973

NATIONAL AERONAUTICS AND SPACE ADMINISTRATION

LANGLEY RESEARCH CENTER, HAMPTON, VIRGINIA 23665

1. Report No.	2. Government Accession No.	3. Recipient's Catalog No.
TM X-71976		

4. Title and Subtitle	5. Report Date
THE EFFECT OF ABLATION INJECTION ON RADIATIVE AND CONVECTIVE HEATING	June 1974
	6. Performing Organization Code
7. Author(s)	8. Performing Organization Report No.
James N. Moss	
9. Performing Organization Name and Address	10. Work Unit No.
Langley Research Center Hampton, VA 23665	11. Contract or Grant No.
	13. Type of Report and Period Covered
12. Sponsoring Agency Name and Address	Technical Memorandum
NASA Langley Research Center Hampton, VA 23665	14. Sponsoring Agency Code

15. Supplementary Notes

Article proposed for publication in the Proceedings of the 10th Anniversary Meeting of the Society of Engineering Science, 1974

16. Abstract

A viscous shock-layer analysis for calculating high energy equilibrium flow fields about blunt axisymmetric bodies is applied to the problem of massive ablation injection with radiation transport. A nongray radiation model is used that accounts for both line and continuum radiation. The solution method is direct and provides both stagnation and downstream solutions. Results for shock heated air show that phenolic-nylon injection is substantially more effective in reducing the wall radiant flux than air injection. Also, for large included body angles, the wall radiative flux and the coupled phenolic-nylon injection rate do not continue to decrease with increasing distance downstream.

17. Key Words (Suggested by Author(s)) (STAR category underlined)	18. Distribution Statement
Radiative viscous flows Ablation Continuum radiation Line radiation Equilibrium Mass injection Shock layer	Unclassified - unlimited

19. Security Classif. (of this report)	20. Security Classif. (of this page)	21. No. of Pages	22. Price*
Unclassified	Unclassified	7	$3.00

*Available from { The National Technical Information Service, Springfield, Virginia 22151
STIF/NASA Scientific and Technical Information Facility, P.O. Box 33, College Park, MD 20740

THE EFFECT OF ABLATION INJECTION ON RADIATIVE AND CONVECTIVE HEATING

James N. Moss
NASA Langley Research Center, Hampton, Va., 23365

ABSTRACT

A viscous shock-layer analysis for calculating high energy equilibrium flow fields about blunt axisymmetric bodies is applied to the problem of massive ablation injection with radiation transport. A nongray radiation model is used that accounts for both line and continuum radiation. The solution method is direct and provides both stagnation and downstream solutions. Results for shock heated air show that phenolic-nylon injection is substantially more effective in reducing the wall radiant flux than air injection. Also, for large included body angles, the wall radiative flux and the coupled phenolic-nylon injection rate do not continue to decrease with increasing distance downstream.

INTRODUCTION

The flow field about planetary entry vehicles is very complex because of the many interactions that occur between ablation injection, radiation transfer, and viscous and diffusion effects. In addition, no experimental data exist which fully duplicate the thermodynamic environment for planetary entry regimes or how the environment interacts with the thermal protection material. Consequently, rigorous numerical analysis of high energy flow fields is essential; essential to the understanding of the basic mechanisms involved in energy transport and to the design of adequate thermal protection systems.

Almost all existing radiative viscous flow analyses are limited to stagnation solutions. However, Sutton (Ref. [1]) and Chou (Ref. [2]) have recently presented downstream solutions for viscous radiating flows. Sutton's analysis is a direct method and is applicable for zero to moderate mass injection while Chou's analysis accounts for massive blowing but is an indirect method.

A rigorous viscous shock-layer analysis for calculating high energy equilibrium flow fields about blunt axisymmetric bodies at zero degree angle of attack is presented herein. The present analysis, based on the analysis developed by Davis (Ref. [3]) for a perfect gas, includes mass injection, radiation transfer, diffusion, and viscous effects. The analysis is direct and provides both stagnation and downstream solution for all levels of blowing. Radiation transfer is calculated with a nongray radiation model that accounts for line and continuum radiation. Results are presented for earth entry conditions to demonstrate the

essential features of this analysis. Particular emphasis is given to the effects of mass injection on the stagnation and downstream flow. Results for both specified and coupled mass injection are presented. The injectants considered are the species for both air and a phenolic-nylon ablator. This is the first direct analysis that provides nonsimilar downstream solutions for radiative viscous flows for all levels of blowing.

ANALYSIS

The viscous shock-layer equations for an equilibrium multicomponent gas mixture are developed in References [4] and [5]. The same viscous shock-layer equations are solved in the present study with the addition of radiation transport. The nondimensional equations in a body oriented coordinate system (Fig. 1) are:

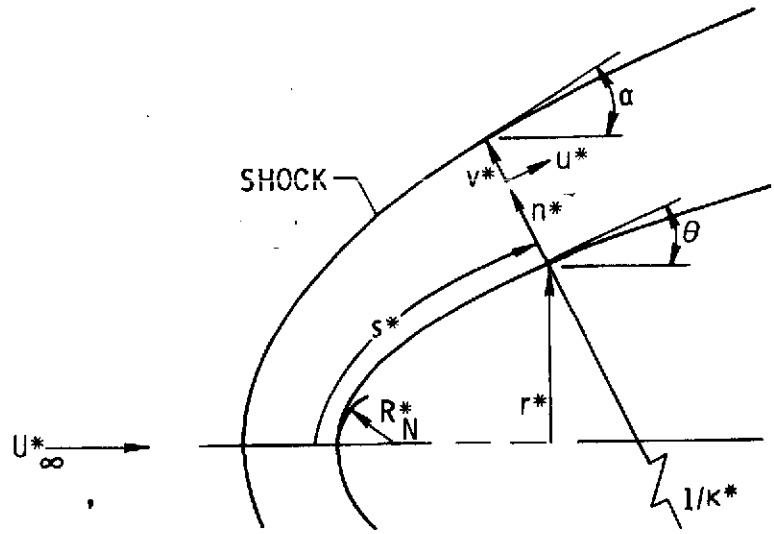

Figure 1. Coordinate system.

Global continuity:

$$\frac{\partial}{\partial s}\left[(r + n\cos\theta)^j \rho u\right] + \frac{\partial}{\partial n}\left[(1 + n\kappa)(r + n\cos\theta)^j \rho v\right] = 0 \qquad (1)$$

s-momentum:

$$\rho\left(\frac{u}{1+n\kappa}\frac{\partial u}{\partial s} + v\frac{\partial u}{\partial n} + \frac{uv\kappa}{1+n\kappa}\right) + \frac{1}{1+n\kappa}\frac{\partial p}{\partial s} = \epsilon^2\left\{\frac{\partial}{\partial n}\left[\mu\left(\frac{\partial u}{\partial n} - \frac{u\kappa}{1+n\kappa}\right)\right] + \mu\left(\frac{2\kappa}{1+n\kappa} + \frac{j\cos\theta}{r+n\cos\theta}\right)\left(\frac{\partial u}{\partial n} - \frac{u\kappa}{1+n\kappa}\right)\right\} \qquad (2)$$

n-momentum:

$$\rho\left(\frac{u}{1+n\kappa}\frac{\partial v}{\partial s} + v\frac{\partial v}{\partial n} - \frac{u^2\kappa}{1+n\kappa}\right) + \frac{\partial p}{\partial n} = 0 \qquad (3)$$

Energy:

$$\rho\left(\frac{u}{1+n\kappa}\frac{\partial H}{\partial s} + v\frac{\partial H}{\partial n}\right) - v\frac{\partial p}{\partial n} + \frac{\rho\kappa u^2 v}{1+n\kappa} = \epsilon^2\left[\frac{\partial \Phi}{\partial n} + \Phi\left(\frac{\kappa}{1+n\kappa} + \frac{j\cos\theta}{r+n\cos\theta}\right)\right] - Q \qquad (4)$$

Elemental continuity:

$$\rho\left(\frac{u}{1+n\kappa}\frac{\partial\tilde{C}_l}{\partial s}+v\frac{\partial\tilde{C}_l}{\partial n}\right)=\frac{\epsilon^2}{(1+n\kappa)(r+n\cos\theta)^j}\left\{\frac{\partial}{\partial n}\left[(1+n\kappa)(r+n\cos\theta)^j\frac{\mu}{N_{Sc}}\frac{\partial\tilde{C}_l}{\partial n}\right]\right\} \tag{5}$$

State:

$$p=\rho TR^*/\bar{M}^*C^*_{p,\infty} \tag{6}$$

where

$$\left.\begin{aligned}&\epsilon=\sqrt{\frac{\mu^*_{ref}}{\rho^*_\infty U^*_\infty R^*_N}},\quad H\equiv h+\frac{u^2}{2},\quad \tilde{C}_l=\sum_{i=1}^{N}\delta_{il}\frac{M^*_l}{M^*_i}C_i,\\ &\Phi=\frac{\mu}{N_{Pr}}\left[\frac{\partial H}{\partial n}+(N_{Le}-1)\sum_{i=1}^{N}h_i\frac{\partial C_i}{\partial n}\right.\\ &\qquad\left.+(N_{Pr}-1)\,u\frac{\partial u}{\partial n}-\frac{N_{Pr}\kappa u^2}{1+n\kappa}\right]\end{aligned}\right\} \tag{7}$$

and Q is the divergence of the radiative flux ($Q^*R^*_N/\rho^*_\infty u^{*3}_\infty$). The superscript * denotes dimensional quantities while j has a value of one for an axisymmetric body and zero for a two-dimensional body. The bar denotes mixture values while the subscripts i and l denote species and elements, respectively. The quantity h is the static enthalpy ($h^*/\rho^*_\infty u^{*2}_\infty$), ρ the density (ρ^*/ρ^*_∞), p the pressure ($p^*/\rho^*_\infty u^{*2}_\infty$), μ the viscosity (μ^*/μ^*_{ref}), $\tilde{C}_l$ the elemental mass fraction, C_i the species mass fraction, M^* the molecular weight, δ_{il} the number of atoms of element l in species i, N the total number of species, R^* the universal gas constant, C^*_p the specific heat, and N_{Pr}, N_{Le}, and N_{Sc} the Prandtl, Lewis, and Schmidt numbers, respectively. The reference viscosity is the viscosity evaluated at the reference temperature $u^{*2}_\infty/C_{p,\infty}$.

The boundary conditions at the shock are calculated by using the Rankine-Hugoniot relations. At the wall, the no slip and no temperature jump boundary conditions are used; consequently, $u_w = 0$. The wall temperature and mass injection rate are either specified or calculated. For the calculated conditions, the mass injection rate is determined from an energy balance at the flow-field-ablator interface. The coupled mass injection rate and surface temperature are calculated by iterating the solution of the governing flow-field equations and the boundary conditions.

The total heat transferred to the surface boundary is given, in nondimensional form, as

$$q_T = q + q_r \tag{8a}$$

where

$$q=\epsilon^2\left[\left(K\frac{\partial T}{\partial n}-\sum_{i=1}^{N}J_ih_i\right)\right]_w+\dot{m}\sum_{i=1}^{N}\left[(C_ih_i)_- -(C_ih_i)_w\right] \tag{8b}$$

The quantity K is the mixture frozen thermal conductivity $(K^*/\mu^*_{ref} C^*_{p,\infty})$, J_i the diffusion mass flux of species i $(J_i^* R_N^*/\mu^*_{ref})$, and $\dot{m}$ the mass injection rate $[(\rho^* v^*)_w/(\rho^* u^*)_\infty]$. The subscripts w and - denote quantities at the surface boundary and adjacent but below the surface boundary, respectively. The radiative flux, $q_r = q_r^*/\rho_\infty^* u_\infty^{*3}$, and the divergence of the radiative flux, Q, are calculated with the radiation transport model LRAD - 3, as presented in Reference [6]. The radiation transport model is an extended version of a coupled line and continuum model that was originally developed by Wilson (Ref. [7]). The LRAD - 3 radiation model accounts for the effects of nongray self-absorption, radiative cooling, and the contribution of atomic line radiation. Twelve continuum frequency bands and nine line bands are used. The species considered for determining the radiation transport are: C, H, N, and O for both continuum and lines and CO, C_2, C_3, O_2, H_2, C_2H, and e^- for continuum. Details of the radiation transport analysis are given in References [6] and [7] and, therefore, will not be reproduced here.

The equilibrium composition is determined by a free energy minimization calculation as developed in Reference [8]. Thermodynamic and transport properties are calculated for each species. In this study, the binary diffusion coefficient is set equal to the diffusion coefficient for atomic carbon diffusing into atomic nitrogen.

The method of solving the governing equations and boundary conditions is discussed in detail in Reference [5]; therefore, only a brief overview of the solution procedure is presented. The governing equations are written in finite-difference form by using Taylor's series expansions. A variable grid spacing is used in both the tangential and normal directions to the surface so that the grid spacing can be made small in the region of large gradients. The order of the truncation terms neglected are Δs and either $\Delta\eta_n \Delta\eta_{n-1}$ or $(\Delta\eta_n - \Delta\eta_{n-1})$, where $\eta = n/n_s$. The governing equations are uncoupled and the dependent variables are solved one at a time at any body station in the following sequence: Rankine-Hugoniot equations to obtain the shock conditions, material response for T_w and $\dot{m}_w$, elemental equations $\tilde{C}_l$, radiation transport for Q, energy equation for H, equilibrium chemistry for C_i and T, s-momentum for u, global continuity for n_s and v, n-momentum for p, and the equation of state for ρ. The solution is iterated until convergence is achieved. The solution advances to the next body station and uses the previous converged solution profiles as initial values for starting the solution at the new body station. This procedure is repeated until a solution pass is obtained. In the first solution pass, it is necessary to make some approximations (see Ref. [5]). These approximations are then removed by iterating the global solution. Two solution passes are generally sufficient. This solution procedure is programed for the CDC 6600 computer.

RESULTS AND DISCUSSION

To demonstrate the essential features of the analysis, results are presented for the following earth entry conditions: velocity = 15.24 km/s and altitude = 62.2 km. The body is a hyperboloid with a total included angle of 120° and a nose radius of 0.305 m. For these conditions, the free-stream Reynolds number is 67,850 and the stagnation shock pressure and temperature are 0.5 atm and 14,700 K, respectively. Mass injection rates, $\dot{m}$, from 0. to 0.60 are considered. Results for both air and phenolic-nylon injection are presented. For air, seven chemical species are used: O, O_2, O^+, N, N_2, N^+, and e^-. For phenolic-nylon, 20 chemical species are used; the seven used for air plus C, C_2, C_3, CO, CN, C_2H, C_3H, C_4H, C_2H_2, C^+, H, H_2, and HCN. The present analysis can be easily modified for planetary atmospheres other than earth by including thermodynamic, transport, and radiative property data for the necessary species that are not presently accounted for.

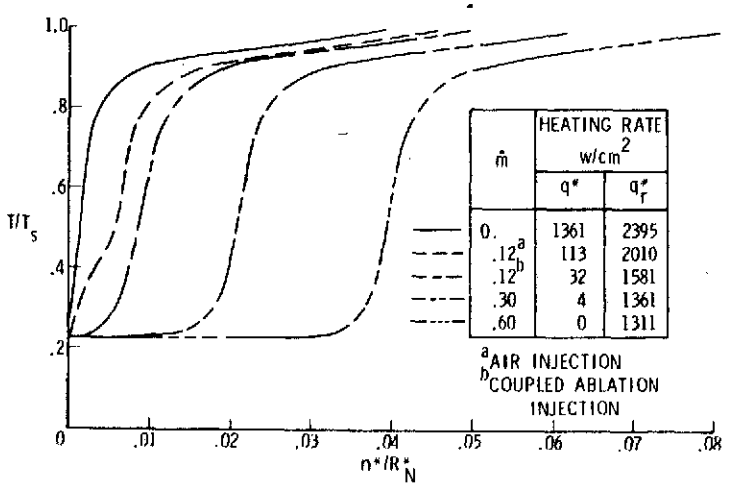

Figure 2. Stagnation temperature profiles for various injection rates.

Figure 2 shows the effect of mass injection on stagnation temperature profiles. Both coupled and arbitrary injection are considered. The injection rate of 0.12 is the coupled mass injection rate for a phenolic-nylon ablator. At this point in the trajectory, the mass injection is sufficient to cause a 98% reduction in q^* and a 34% reduction in q_r^*. For phenolic-nylon injection, the specific heat of the gas is much greater near the wall and the radiation flux toward the wall is attenuated much more than for the corresponding air injection rate. Consequently, the phenolic-nylon injection has a much larger effect on temperature profile and surface heating than air injection, as shown in Figure 2. For air injection of 0.12, the heating reduction is 92% for q^* and 16% for q_r^*. For phenolic-nylon injection rates in excess of the coupled injection value, only small additional reductions in heating occur.

For large injection rates, the problem of numerical instabilities is characteristic of most, if not all, analyses that have been developed. For example, the analysis described in Reference [9] was unable to obtain a converged solution to the energy equation for an injection rate of 0.2. However, with the present analysis, a converged solution is obtained for injection rates substantially in excess of 0.2, as shown in Figure 2.

Figure 3 presents the surface heating rate and mass injection distributions where the mass injection from a phenolic-nylon ablator is coupled with the radiating flow-field solution. For the body shape considered and because the shock thickens with distance downstream, the radiative heating and mass injection do not continue to decrease with increasing distance downstream. Figure 4 shows the tangential velocity profiles for the stagnation and downstream locations. These results show very clearly

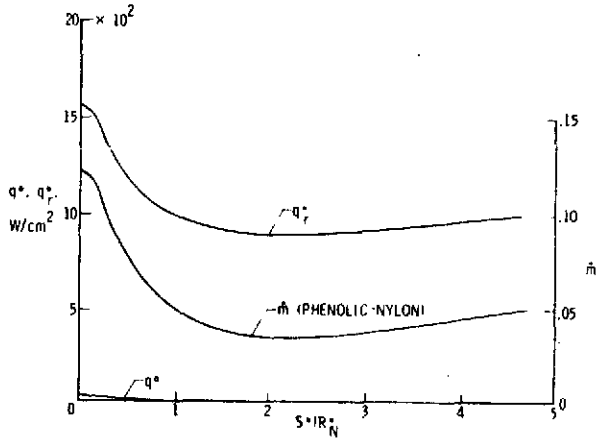

Figure 3. Shock-layer results with coupled ablation injection.

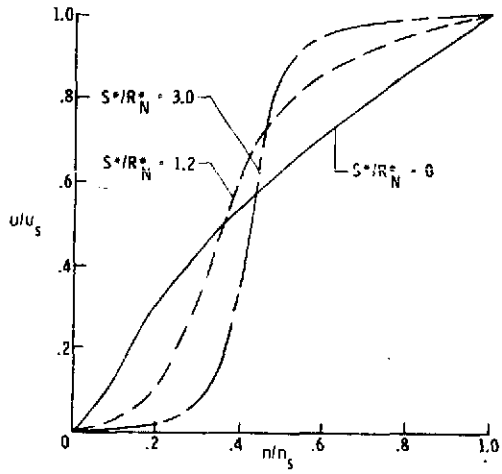

Figure 4. Tangential velocity profiles for coupled ablation injection.

the nonsimilar behavior of the flow field. Also, note that the viscous effects along the stagnation streamline are evident throughout the shock layer. Downstream, however, the viscous effects are confined to a small segment of the shock-layer thickness.

The spectral details of the radiation flux at the wall are shown for the continuum and line radiation in Figure 5. A comparison of the surface spectral flux with and without injection are made. The results show that for both continuum and line radiation, the phenolic-nylon injection causes a large attenuation of the ultraviolet radiation.

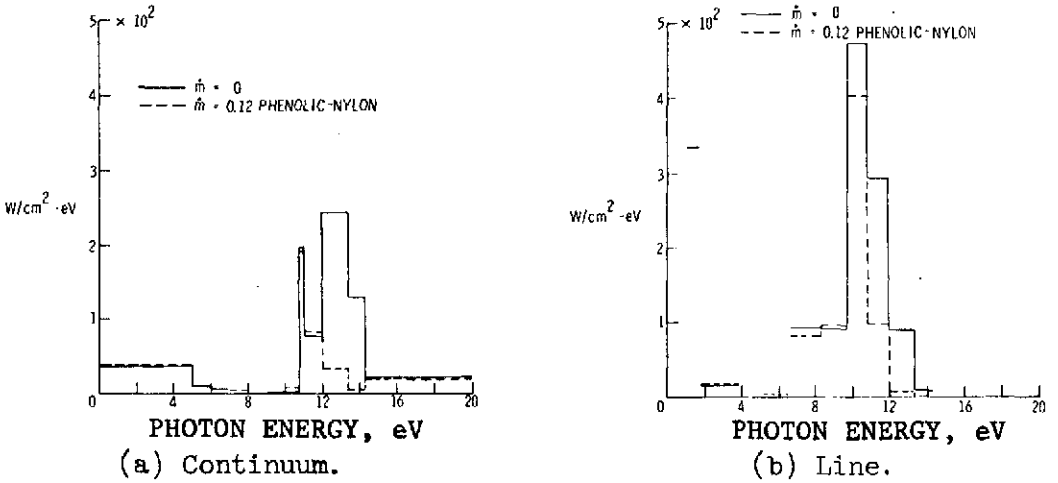

Figure 5. Comparison of wall radiation with and without mass injection.

REFERENCES

[1]Kenneth Sutton, "Fully Coupled Nongray Radiating Gas Flows with Ablation Product Effects About Planetary Entry Bodies," AIAA Paper No. 73-672, July 1973.

[2]Y. S. Chou, "Effect of Downstream Massive Blowing on Jovian Entry Heating," AIAA Paper No. 73-717, July 1973.

[3]R. T. Davis, "Numerical Solution of the Hypersonic Viscous Shock-Layer Equations," AIAA J., Vol. 8, May 1970, pp. 843-851.

[4]James N. Moss, "Solutions for Reacting and Nonreacting Viscous Shock Layers with Multicomponent Diffusion and Mass Injection," Ph.D. Thesis, Virginia Polytechnic Institute and State University, 1971.

[5]James N. Moss, "Reacting Viscous Shock-Layer Solutions with Multicomponent Diffusion and Mass Injection," NASA TR R-411 (to be published).

[6]Carl D. Engel, Richard C. Farmer, and Ralph W. Pike, "Ablation and Radiation Coupled Viscous Hypersonic Shock Layers," NASA CR-112306, 1971.

[7]K. H. Wilson, "Stagnation Point Analysis of Coupled Viscous-Radiating Flow with Massive Blowing," NASA CR-1548, 1970.

[8]C. W. Stroud and Kay L. Brinkley, "Chemical Equilibrium of Ablation Materials Including Condensed Species. NASA TN D-5391, 1969.

[9]L. B. Garrett, G. L. Smith, and J. N. Perkins, "An Implicit Finite-Difference Solution to the Viscous Shock Layer Including the Effects of Radiation and Strong Blowing," NASA TR R-388, 1972.